Modeling, Analysis, and Simulation of Nonfrequency-Selective Mobile Radio Channels with Asymmetrical Doppler Power Spectral Density Shapes

Matthias Pätzold, *Member, IEEE,* Ulrich Killat, *Member, IEEE,* Yingchun Li, and Frank Laue

***Abstract*— What terrestrial and satellite land mobile radio channels have in common is that they are usually assumed to be nonfrequency selective. For such fading channels, a highly flexible analytical model is presented. Our model takes into account short-term fading with superimposed long-term lognormal variations of the local mean value of the received signal. It is assumed that the introduced complex stochastical process, which is used for modeling the short-term fading behavior, has a Doppler power spectral density with an asymmetrical shape. Closed solutions are presented showing the influence of asymmetrical Doppler power spectral density shapes on the statistical properties of the proposed channel model. A numerical optimization procedure is shown for the optimization of the model parameters in order to fit the statistics of the analytical model [amplitude probability density function (pdf), level-crossing rate (LCR), and average duration of fades (ADF)] to measurement results of an equivalent land mobile satellite channel for light and heavy shadowing environments. Finally, from the analytical model, an efficient simulation model is derived that enables the simulation of such realistic land mobile satellite channel scenarios on a digital computer.**

***Index Terms*— Average duration of fades, extended Suzuki process, level-crossing rate, nonfrequency-selective fading.**

I. Introduction

THE MOBILE radio channel is a propagation medium that is characterized by wave phenomena like reflection, diffraction, scattering, and absorption. In principle, the exact knowledge of the geometric dimensions and electromagnetic properties of the physical environment allows a precise description of all these propagation phenomena and enables the derivation of realistic and accurate channel models. But, this procedure requires, unfortunately, an extremely large mathematical effort so that many scientists feel obliged to reduce the complex physical propagation process to the main features characterizing the fundamental statistical properties of the mobile radio channel. In this manner, the problem reduces to the discovery and description of appropriate stochastic model processes and its accurate adaption to measurement data of real-world mobile radio channels simply by fitting the model parameters. Thus, such semi-empirical procedures are based on theoretical model assumptions and on measurement data.

The digital transmission of signals over land mobile radio channels is affected by two different kinds of fading effects: short-term and long-term fading. The short-term fading is caused by the local multipath propagation and follows in urban environments, often closely, a Rayleigh distribution [1], [2]. On the other hand, the long-term fading is due to shadowing and is usually lognormally distributed [3]–[5]. Suzuki [6] and Hansen *et al.* [7] proposed a statistical model for the envelope of the received mobile radio signal that can be represented by a Rayleigh distribution with a lognormally-varying local mean. Today, the Suzuki process [6], i.e., the product process of a Rayleigh and a lognormal process, is a widely accepted and suitable statistical model for large classes of land mobile radio channels, provided that the influence of a direct line-of-sight (LOS) component can be neglected. In most cases, the underlying Rayleigh process is regarded as the envelope of a complex-valued Gaussian noise process, where it is assumed that its inphase and quadrature components are statistically independent. But such an assumption does not always meet the real-world conditions in multipath wave propagation. Therefore, modified Suzuki processes have been introduced [8], [9], where the components generating the Rayleigh process are allowed to be cross correlated. In [8] and [9], the statistical properties of the modified Suzuki process have been investigated, and it has been shown that the proposed type of cross correlation influences the higher order statistics [level-crossing rate (LCR) and average duration of fades (ADF)], but not the probability density function (pdf) of the envelope.

A statistical channel model based on a product process of a Rice and lognormal process was proposed in [10] for nongeostationary satellite channels, such as low-earth and medium-earth orbit channels. This statistical model has been extended in [11] in such a way that the two Gaussian processes describing the Rice process are allowed to be cross correlated. The resulting extended Suzuki process contains the (modified) Suzuki process as a special case.

In this paper, a new type of extended Suzuki process is introduced, which enables, due to its high flexibility, a better

Manuscript received December 1, 1995; revised June 18, 1996.

M. Pätzold is with the Technical University of Hamburg-Harburg, Department of Digital Communication Systems, Hamburg, Germany (e-mail: paetzold@tu-harburg.d400.de).

U. Killat, Y. Li, and F. Laue are with the Technical University of Hamburg-Harburg, Department of Digital Communication Systems, Hamburg, Germany.

Publisher Item Identifier S 0018-9545(97)03140-X.

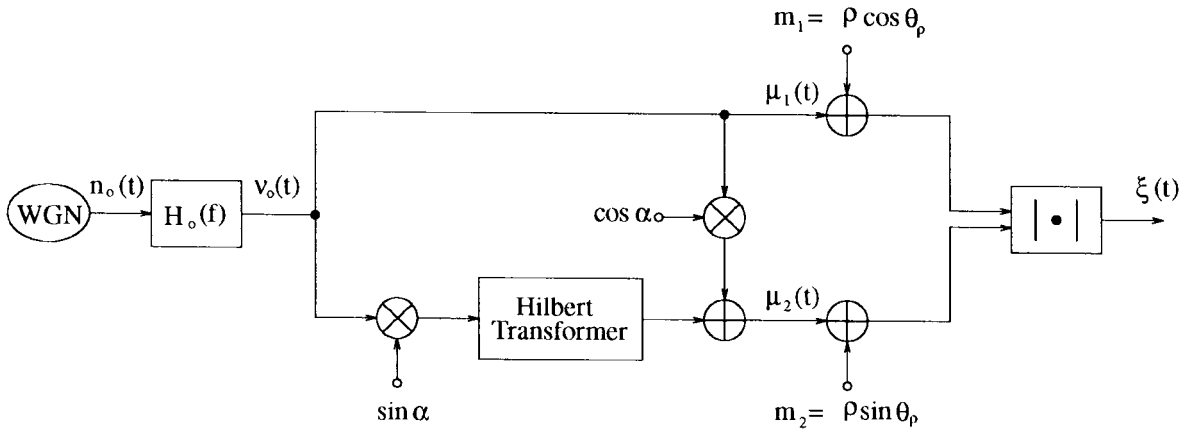

Fig. 1. Analytical model for a stochastical process with underlying cross-correlated quadrature components, where $H_o(f) = \sqrt{S_{\nu_o\nu_o}(f)}$.

statistical fitting to real-world mobile satellite channels than other statistical channel models, such as the models proposed in [11]–[13].

We have organized the paper as follows. In Section II, a new complex stochastical process is introduced, whose inphase and quadrature components are derived from a single colored Gaussian noise process. It will be shown that the distribution of the envelope of that new complex process contains the Rice, Rayleigh, and one-sided Gaussian distribution as special cases. Besides the derivation of analytical expressions for the amplitude and phase pdf, closed-form expressions for the LCR and the ADF are also given. In Section III, we will recapitulate the statistical properties of lognormal processes as far as it is of further importance for the rest of the paper. Section IV investigates the statistical properties of the proposed new extended Suzuki process, such as the pdf of the amplitude, LCR, and ADF. Finally, in Section V, we will demonstrate the high performance of the proposed procedure by fitting the statistics (amplitude pdf, LCR, and ADF) of the analytical model to the corresponding measurement data of an equivalent land mobile satellite channel for light and heavy shadowing environments. Moreover, we present an efficient simulation model, whose statistical properties are in excellent conformity with the underlying analytical model. In Section VI, we conclude the paper with a summary and some discussions of the results.

II. Modelling of Short-Term Fading Variations

Throughout the paper, we assume that the mobile channel is nonfrequency-selective, i.e., the coherence bandwidth of the mobile channel is large in comparison to the bandwidth of the transmitted signal.

The stochastical model that we propose for the modeling of the short-term fading variations of large classes of nonfrequency-selective fading channels is depicted in Fig. 1. In this section, the statistical properties of that analytical model will be investigated. From Fig. 1, we observe that a single colored zero mean Gaussian noise process $\nu_o(t)$ is used to produce a complex Gaussian noise process

$$\mu(t) = \mu_1(t) + j\mu_2(t) \tag{1}$$

with cross-correlated quadrature components $\mu_1(t)$ and $\mu_2(t)$. Our proposed stochastical model takes into consideration a direct LOS component of the form

$$m_\rho = m_1 + jm_2 = \rho e^{j\theta_\rho} \tag{2}$$

where ρ denotes the amplitude and θ_ρ is the phase of the LOS component. We note that m_ρ is supposed to be independent of time, i.e., the Doppler frequency of the LOS component is equal to zero. From the nonzero mean complex Gaussian noise process $\mu_\rho(t) = \mu(t) + m_\rho$, a further stochastical process $\xi(t)$ can be obtained by taking the absolute value

$$\xi(t) = |\mu_\rho(t)| = \sqrt{(\mu_1(t) + m_1)^2 + (\mu_2(t) + m_2)^2}\ . \tag{3}$$

We will see subsequently that the above stochastical process $\xi(t)$, with underlying cross-correlated quadrature components, contains the Rice, Rayleigh, and one-sided Gaussian processes as special cases and can therefore be considered as a generalization of those classical processes. Of course, that model is valid only for short distances covered by the vehicle. In such a case, the local mean of the received signal strength, i.e., the time-average value of $\xi(t)$ over a few tens of wavelengths, is approximately a constant quantity. For longer distances, the local mean itself is a random variable, and a more precise model can be obtained by multiplying the stochastical process $\xi(t)$ with a lognormal process, which results in a so-called extended Suzuki process (see Section IV). Such a model can be used for the simulation of the fading statistics of real-world land mobile satellite channels, as will be shown in Section V.

A widely accepted Doppler power spectral density (PSD) function for mobile fading channel models is the Jakes PSD [14]

$$S_{JJ}(f) = \begin{cases} \frac{\sigma_o^2}{\pi f_{\max}\sqrt{1-(f/f_{\max})^2}}, & |f| < f_{\max} \\ 0, & |f| \geq f_{\max} \end{cases} \tag{4}$$

where $f_{\max}$ is the maximum Doppler frequency and σ_o^2 denotes the mean power, i.e., $\sigma_o^2 = \int_{-\infty}^{\infty} S_{JJ}(f)df$. The symmetrical shape of the Jakes PSD $S_{JJ}(f)$ [see Fig. 2(a)] is a direct consequence of the idealized assumption that the incoming directions of the received multipath waves are uniformly distributed in the interval $[0, 2\pi)$. If some of the

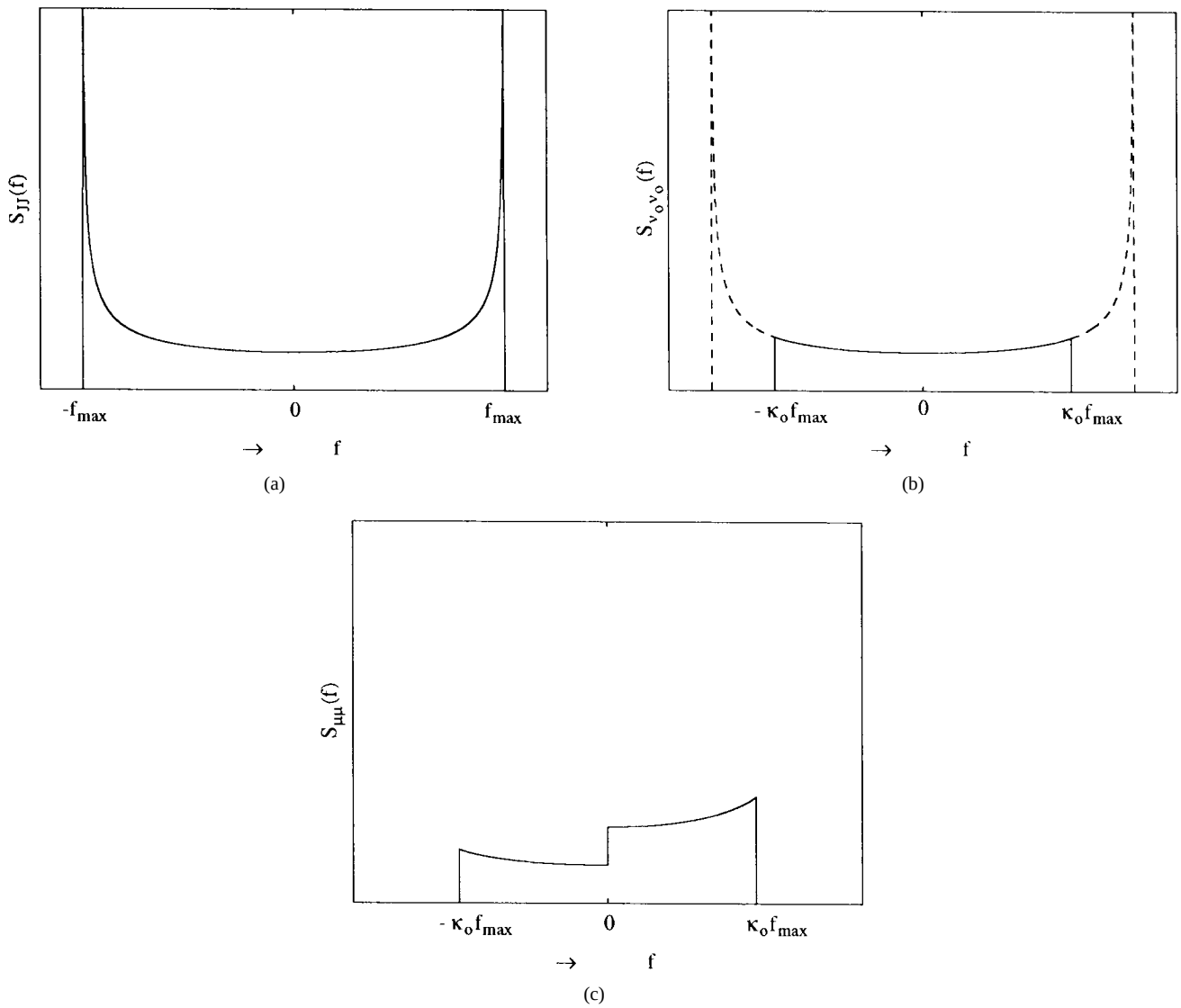

Fig. 2. Diverse Doppler PSD functions: (a) the symmetrical Jakes PSD $S_{JJ}(f)$, (b) the restricted Jakes PSD $S_{\nu_o\nu_o}(f)$, and (c) an asymmetrical PSD $S_{\mu\mu}(f)$.

multipath waves are blocked by obstacles or absorbed by the electromagnetic properties of the physical environment, then, the resulting Doppler PSD of the complex Gaussian noise process $\mu(t)$ becomes asymmetrical.

Now, we will show how to get an asymmetrical Doppler PSD function that takes into account the absorption of all those received multipath waves with negative Doppler frequencies. Moreover, we take into consideration blocking effects in such a manner that the Doppler PSD of the process $\nu_o(t)$, $S_{\nu_0\nu_0}(f)$, has a restricted Jakes PSD characteristic of the form $S_{\nu_0\nu_0}(f) = \text{rect}\,[f/(\kappa_o f_{\max})] \cdot S_{JJ}(f)$, where $0 < \kappa_o \leq 1$ [see Fig. 2(b)].

The following expressions can be derived from Fig. 1:

$$\mu_1(t) = \nu_o(t) \tag{5a}$$

$$\mu_2(t) = \cos\alpha \cdot \nu_o(t) + \sin\alpha \cdot \check{\nu}_o(t) \tag{5b}$$

where the notation $\check{\nu}_o(t)$ in (5b) denotes the corresponding Hilbert transform of the process $\nu_o(t)$ [15] and the parameter $\alpha \in (0, \pi)$ is called the correlation factor, which controls the cross correlation between $\mu_1(t)$ and $\mu_2(t)$. The autocorrelation function $r_{\mu_1\mu_1}(t)$ of the process $\mu_1(t)$ and the cross-correlation function $r_{\mu_1\mu_2}(t)$ of the processes $\mu_1(t)$ and $\mu_2(t)$ can be expressed by the autocorrelation function $r_{\nu_o\nu_o}(t)$ of the process $\nu_o(t)$ and the cross-correlation function $r_{\check{\nu}_o\nu_o}(t)$ of the processes $\check{\nu}_o(t)$ and $\nu_o(t)$ as follows:

$$r_{\mu_1\mu_1}(t) = r_{\mu_2\mu_2}(t) = r_{\nu_o\nu_o}(t) \tag{6a}$$

$$r_{\mu_1\mu_2}(t) = \cos\alpha \cdot r_{\nu_o\nu_o}(t) - \sin\alpha \cdot r_{\check{\nu}_o\nu_o}(t) \tag{6b}$$

$$r_{\mu_2\mu_1}(t) = \cos\alpha \cdot r_{\nu_o\nu_o}(t) + \sin\alpha \cdot r_{\check{\nu}_o\nu_o}(t). \tag{6c}$$

After some simple algebraic computations, the autocorrelation function[1] and corresponding Doppler PSD function of the complex process $\mu(t)$ can be expressed by

$$r_{\mu\mu}(t) = 2r_{\nu_o\nu_o}(t) - j2\sin\alpha \cdot r_{\check{\nu}_o\nu_o}(t) \tag{7}$$

$$S_{\mu\mu}(f) = 2S_{\nu_o\nu_o}(f) - j2\sin\alpha \cdot S_{\check{\nu}_o\nu_o}(f). \tag{8}$$

Finally, by using the relation $S_{\check{\nu}_o\nu_o}(f) = jsgn(f)S_{\nu_o\nu_o}(f)$, $S_{\mu\mu}(f)$ can be written as a function of $S_{\nu_o\nu_o}(f)$ in the

[1] In this paper, the autocorrelation function of the complex Gaussian noise process $\mu(t)$ is defined by $r_{\mu\mu}(t) = E\{\mu^*(\tau)\mu(t+\tau)\}$, where $E\{\cdot\}$ denotes expectation (statistical averaging).

following way:

$$S_{\mu\mu}(f) = 2[1 + sgn(f)\sin\alpha] \cdot S_{\nu_o\nu_o}(f) \tag{9}$$

which has for $\alpha \in (0, \pi)$ an asymmetrical shape. An example for the Doppler PSD function $S_{\mu\mu}(f)$ is depicted in Fig. 2(c), where for the correlation factor α, the value $\alpha = 19.5°$ has been chosen.

A starting point for the derivation of the statistics of the stochastic process $\xi(t)$ [consider (3)] is the joint pdf (JPDF) of the processes $\xi(t)$, $\dot{\xi}(t)$, $\vartheta(t)$, and $\dot{\vartheta}(t)$, where $\vartheta(t)$ is the phase of the complex process $\mu_\rho(t)$ and the overdot denotes the time derivative. From that JPDF, the pdf of the amplitude $\xi(t)$ and phase $\vartheta(t)$, the LCR, and the ADF can be derived easily. A general procedure for the derivation of JPDF's resulting from complex Gaussian noise processes with cross-correlated quadrature components is described in detail in [11]. Here, we apply that procedure, and we only give the final result [see (10)] and all the relations [see (11a)–(11d)] used to express the JPDF $p_{\xi\dot{\xi}\vartheta\dot{\vartheta}}(z, \dot{z}, \theta, \dot{\theta})$:

$$\begin{aligned} p_{\xi\dot{\xi}\vartheta\dot{\vartheta}}(z, \dot{z}, \theta, \dot{\theta}) &= \frac{z^2}{(2\pi)^2\beta\psi_o\sin^2\alpha} \\ &\cdot e^{-\frac{1}{2\psi_o\sin^2\alpha}[z^2+\rho^2-2z\rho\cos(\theta-\theta_\rho)]} \\ &\cdot e^{\frac{\cos\alpha}{2\psi_o\sin^2\alpha}[z^2\sin 2\theta+\rho^2\sin 2\theta_\rho-2z\rho\sin(\theta+\theta_\rho)]} \\ &\cdot e^{-\frac{1}{2\beta(1+\cos\alpha\cdot\sin 2\theta)}\cdot\left\{\dot{z}-\frac{\dot{\phi}_o[\rho\sin(\theta-\theta_\rho)-\cos\alpha(z\cos 2\theta-\rho\cos(\theta+\theta_\rho))]}{\psi_o\sin\alpha}\right\}^2} \\ &\cdot e^{-\frac{z^2(1+\cos\alpha\cdot\sin 2\theta)}{2\beta\sin^2\alpha}\cdot\left\{\dot{\theta}-\frac{\dot{\phi}_o\sin\alpha[\rho\cos(\theta-\theta_\rho)-z]+\psi_o\dot{z}\cos\alpha\cdot\cos 2\theta}{\psi_o z(1+\cos\alpha\cdot\sin 2\theta)}\right\}^2} \end{aligned} \tag{10}$$

where $z \geq 0$, $-\infty \leq \dot{z} \leq \infty$, $-\pi \leq \theta < \pi$, $-\infty \leq \dot{\theta} \leq \infty$, and

$$\beta = -\ddot{\psi}_o - \dot{\phi}_o^2/\psi_o \tag{11a}$$

$$\psi_o = r_{\mu_1\mu_1}(0) = r_{\mu_2\mu_2}(0) = \frac{2}{\pi}\sigma_o^2\arcsin(\kappa_o) \tag{11b}$$

$$\begin{aligned} \ddot{\psi}_o &= \ddot{r}_{\mu_1\mu_1}(0) = \ddot{r}_{\mu_2\mu_2}(0) \\ &= -2\psi_o(\pi f_{\max})^2\{1 - \mathrm{sinc}[2\arcsin(\kappa_o)]\} \end{aligned} \tag{11c}$$

$$\dot{\phi}_o = \dot{r}_{\check{\nu}_o\nu_o}(0) = -4\sigma_o^2 f_{\max}(1 - \sqrt{1-\kappa_o^2}). \tag{11d}$$

Note that ψ_o represents the mean power of the process $\mu_1(t)$ ($\mu_2(t)$), $\ddot{\psi}_o$ designates the curvature of the autocorrelation function $r_{\mu_1\mu_1}(t)$ ($r_{\mu_2\mu_2}(t)$) at time $t = 0$, and $\dot{\phi}_o$ is the time derivative of the cross-correlation function $r_{\check{\nu}_o\nu_o}(t)$ at time $t = 0$.

In the following two subsections, we derive from the JPDF $p_{\xi\dot{\xi}\vartheta\dot{\vartheta}}(z, \dot{z}, \theta, \dot{\theta})$ the PDF of the amplitude $\xi(t)$ and phase $\vartheta(t)$ as well as the LCR and ADF of the process $\xi(t)$.

A. Amplitude and Phase pdf's

The PDF of the process $\xi(t)$, $p_\xi(z)$, can be derived by solving the integrals

$$p_\xi(z) = \int_{-\infty}^{\infty}\int_{-\pi}^{\pi}\int_{-\infty}^{\infty} p_{\xi\dot{\xi}\vartheta\dot{\vartheta}}(z, \dot{z}, \theta, \dot{\theta})d\dot{z}d\theta d\dot{\theta}, \quad z \geq 0 \tag{12}$$

where $p_{\xi\dot{\xi}\vartheta\dot{\vartheta}}(z, \dot{z}, \theta, \dot{\theta})$ is the JPDF of $\xi(t)$, $\dot{\xi}(t)$, $\vartheta(t)$, and $\dot{\vartheta}(t)$ as given by (10). After substituting (10) into (12), the PDF $p_\xi(z)$ can be expressed as follows:

$$\begin{aligned} p_\xi(z) = &\frac{z}{2\pi\psi_o\sin\alpha}e^{-\frac{z^2+\rho^2}{2\psi_o\sin^2\alpha}}\cdot\int_{-\pi}^{\pi} e^{\frac{z\rho\cos(\theta-\theta_\rho)}{\psi_o\sin^2\alpha}} \\ &\cdot e^{\frac{\cos\alpha}{2\psi_o\sin^2\alpha}[z^2\sin 2\theta+\rho^2\sin 2\theta_\rho-2z\rho\sin(\theta+\theta_\rho)]}d\theta, \\ &z \geq 0. \end{aligned} \tag{13}$$

From (13), we observe that only ψ_o, i.e., the mean power of the processes $\mu_1(t)$, $\mu_2(t)$, as well as α, ρ, and θ_ρ have an influence on the PDF $p_\xi(z)$, but not $\dot{\phi}_o$ and $\ddot{\psi}_o$. Therefore, the PDF $p_\xi(z)$ is not affected by the cross correlation between $\check{\nu}_o(t)$ and $\nu_o(t)$ and is also completely independent of the exact shape of the Doppler PSD function $S_{\nu_o\nu_o}(f)$. The influence of the correlation factor α and the phase of the LOS component θ_ρ on the amplitude PDF $p_\xi(z)$ is shown in Fig. 3(a) and (b), respectively.

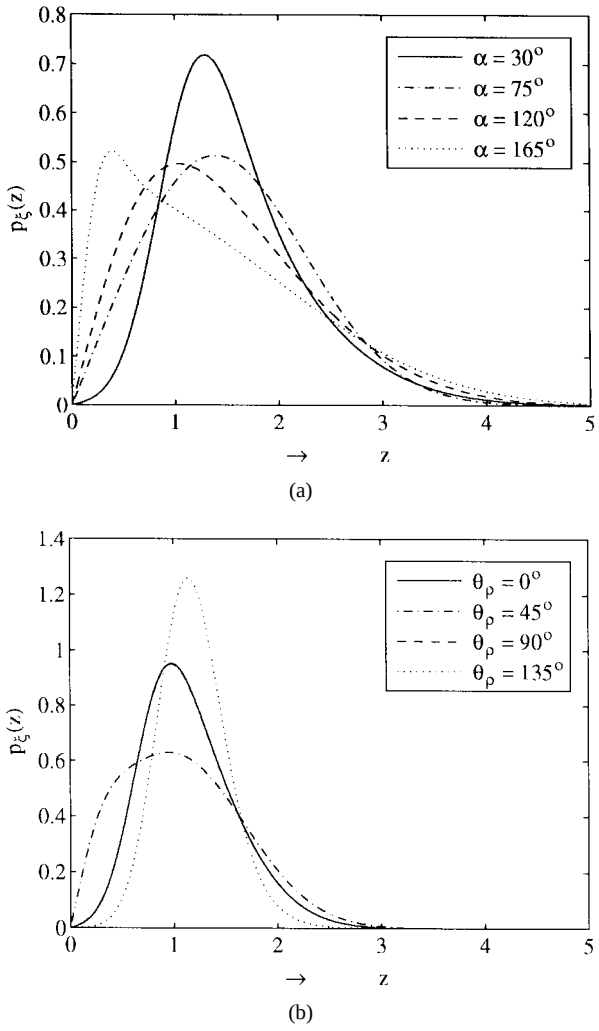

Fig. 3. Theoretical result of the pdf $p_\xi(z)$ as function of: (a) α ($\psi_o = 0.2657$, $\rho = 1$, $\theta_\rho = 127^o$), (b) θ_ρ ($\psi_o = 1$, $\rho = 1$, $\alpha = 45^o$).

The above expression for the PDF $p_\xi(z)$ contains the Rice, Rayleigh, and one-sided Gaussian densities as special cases. Let $\alpha = 90^o$, then (13) reduces to the Rice density [16]

$$p_\xi(z) = \frac{z}{\psi_o}e^{-\frac{z^2+\rho^2}{2\psi_o}}I_o\left(\frac{z\rho}{\psi_o}\right), \qquad z \geq 0 \tag{14}$$

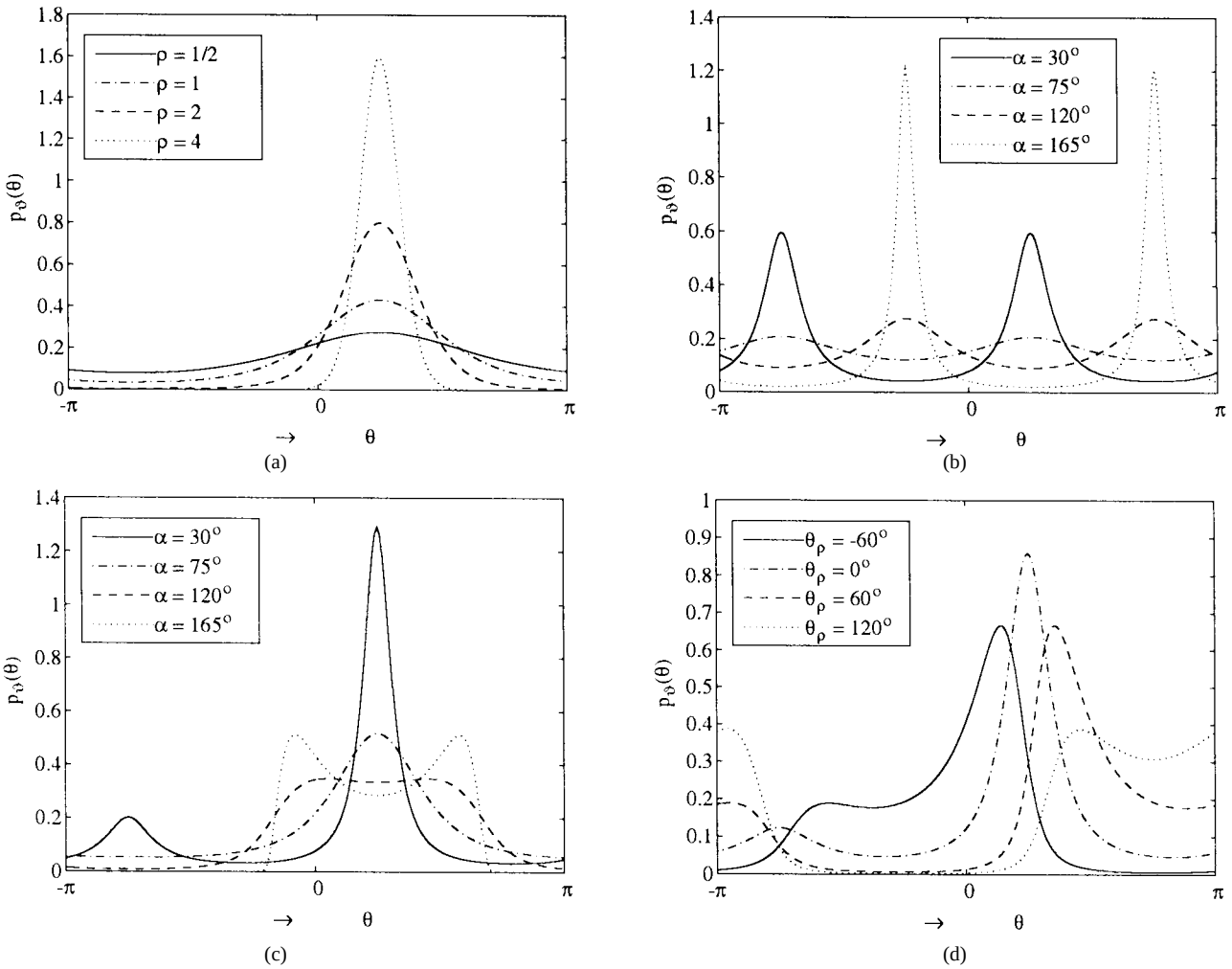

Fig. 4. Theoretical result of the pdf $p_\vartheta(\theta)$ as a function of: (a) ρ ($\psi_o = 1$, $\alpha = 90^o$, and $\theta_\rho = 45^o$), (b) α ($\psi_o = 1$ and $\rho = 0$), (c) α ($\psi_o = 1$, $\rho = 1$, and $\theta_\rho = 45^o$), and (d) θ_ρ ($\psi_o = 1$, $\rho = 1$, and $\alpha = 45^o$).

where $I_o(\cdot)$ denotes the zeroth-order modified Bessel function of the first kind. On the other hand, if $\rho = 0$, i.e., no LOS component is present, then (13) results in the density

$$p_\xi(z) = \frac{z}{\psi_o \sin\alpha} e^{-\frac{z^2}{2\psi_o \sin^2\alpha}} I_o\left(\frac{z^2\cos\alpha}{2\psi_o \sin^2\alpha}\right), \qquad z \geq 0 \tag{15}$$

which yields for $\alpha = 90^o$ the Rayleigh density [15]

$$p_\xi(z) = \frac{z}{\psi_o} e^{-\frac{z^2}{2\psi_o}}, \qquad z \geq 0 \tag{16}$$

and in the limit $\alpha \to 0$, (15) leads to the one-sided Gaussian density

$$p_\xi(z) = \frac{1}{\sqrt{\pi\psi_o}} e^{-\frac{z^2}{4\psi_o}}, \qquad z \geq 0. \tag{17}$$

In a similar way, the PDF of the phase $\vartheta(t)$, $p_\vartheta(\theta)$, can be derived by solving the integrals over the JPDF $p_{\xi\dot{\xi}\vartheta\dot{\vartheta}}(z, \dot{z}, \theta, \dot{\theta})$ according to

$$p_\vartheta(\theta) = \int_{-\infty}^{\infty}\int_{-\infty}^{\infty}\int_0^{\infty} p_{\xi\dot{\xi}\theta\dot{\theta}}(z, \dot{z}, \theta, \dot{\theta})\, dz\, d\dot{z}\, d\dot{\theta}, \quad \theta \in [-\pi, \pi). \tag{18}$$

This yields the following expression:

$$p_\vartheta(\theta) = \frac{\sin\alpha}{2\pi(1 - \cos\alpha \cdot \sin 2\theta)} \cdot e^{-\frac{\rho^2(1-\cos\alpha\cdot\sin 2\theta_\rho)}{2\psi_o \sin^2\alpha}} \cdot \{1 + \sqrt{\pi} f(\theta) e^{f^2(\theta)}[1 + \operatorname{erf}(f(\theta))]\}, \quad \theta \in [-\pi, \pi) \tag{19a}$$

where

$$f(\theta) = \frac{\rho[\cos(\theta - \theta_\rho) - \cos\alpha \cdot \sin(\theta + \theta_\rho)]}{\sin\alpha\sqrt{2\psi_o(1 - \cos\alpha \cdot \sin 2\theta)}} \tag{19b}$$

and $\operatorname{erf}(\cdot)$ denotes the error function. Equation (19) also shows that neither $\dot{\phi}_o$ nor $\ddot{\psi}_o$ have an influence on $p_\vartheta(\theta)$. Observe that for a correlation factor of $\alpha = 90°$, the phase PDF $p_\vartheta(\theta)$ is identical with the phase PDF of Rice processes with uncorrelated quadrature components $\mu_1(t)$ and $\mu_2(t)$ [11], i.e.,

$$p_\vartheta(\theta) = \frac{e^{-\frac{\rho^2}{2\psi_o}}}{2\pi}\left\{1 + \sqrt{\frac{\pi}{2\psi_o}}\rho\cos(\theta - \theta_\rho) e^{\frac{\rho^2\cos^2(\theta-\theta_\rho)}{2\psi_o}}\left[1 + \operatorname{erf}\left(\frac{\rho\cos(\theta - \theta_\rho)}{\sqrt{2\psi_o}}\right)\right]\right\} \tag{20}$$

where $\theta \in [-\pi, \pi)$. If $\rho = 0$ and $\alpha = 90^o$, then $p_\vartheta(\theta)$ is uniformly distributed in the interval $[-\pi, \pi)$.

The influence of the parameters α, ρ, and θ_ρ on the phase PDF $p_\vartheta(\theta)$ is shown in Fig. 4.

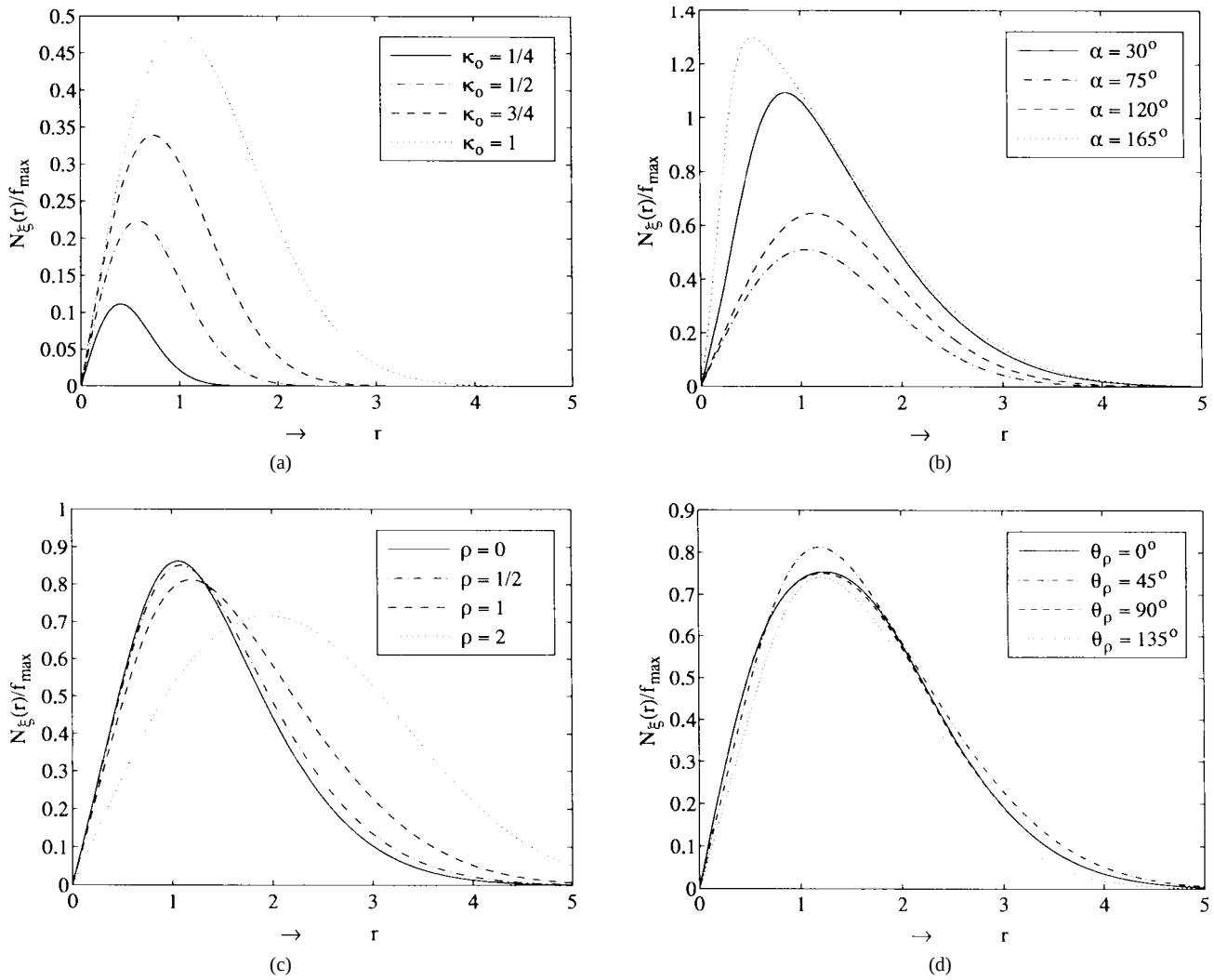

Fig. 5. Theoretical result of the normalized LCR $N_\xi(r)/f_{\max}$ as a function of: (a) κ_o ($\sigma_o = 1$, $\alpha = 45°$, and $\rho = 0$), (b) α ($\psi_o = 1$, $\kappa_o = 1$, and $\rho = 0$), (c) ρ ($\psi_o = 1$, $\kappa_o = 1$, $\alpha = 45°$, and $\theta_\rho = 45°$), and (d) θ_ρ ($\psi_o = 1$, $\kappa_o = 1$, $\alpha = 45°$, and $\rho = 1$).

B. LCR and ADF

The LCR $N_\xi(r)$ is the average number of crossings per second at which the envelope $\xi(t)$ crosses a specified signal level r with a positive slope. In general, the LCR $N_\xi(r)$ for any wide-sense stationary random process is defined by [16]

$$N_\xi(r) = \int_0^\infty \dot{z} p_{\xi\dot{\xi}}(r, \dot{z}) d\dot{z} \tag{21}$$

where $p_{\xi\dot{\xi}}(r, \dot{z})$ is the JPDF of $\xi(t)$ and $\dot{\xi}(t)$ at the same time and at the level $z = r$. From (10), we obtain after some computations for that JPDF the following integral expression:

$$\begin{aligned} p_{\xi\dot{\xi}}(z, \dot{z}) &= \frac{z}{(2\pi)^{3/2}\psi_o\sqrt{\beta}\sin\alpha} e^{-\frac{z^2+\rho^2}{2\psi_o \sin^2\alpha}} \int_{-\pi}^{\pi} \frac{1}{\sqrt{1+\cos\alpha\cdot\sin 2\theta}} \\ &\cdot e^{\frac{z\rho\cos(\theta-\theta_\rho)}{\psi_o\sin^2\alpha}} \cdot e^{\frac{\cos\alpha}{2\psi_o\sin^2\alpha}[z^2\sin 2\theta+\rho^2\sin 2\theta_\rho - 2z\rho\sin(\theta+\theta_\rho)]} \\ &\cdot e^{-\frac{1}{2\beta(1+\cos\alpha\cdot\sin 2\theta)}\left\{\dot{z}-\frac{\dot{\phi}_o[\rho\sin(\theta-\theta_\rho)-\cos\alpha(z\cos 2\theta-\rho\cos(\theta+\theta_\rho))]}{\psi_o\sin\alpha}\right\}^2} \\ &\cdot d\theta \end{aligned} \tag{22}$$

where $z \geq 0$ and $-\infty \leq \dot{z} \leq \infty$.

The LCR $N_\xi(r)$ of the signal envelope $\xi(t)$ can now be derived by substituting (22) into (21). The final result is given by

$$\begin{aligned} N_\xi(r) &= \frac{r\sqrt{\beta}}{(2\pi)^{3/2}\psi_o\sin\alpha} e^{-\frac{r^2+\rho^2}{2\psi_o\sin^2\alpha}} \int_{-\pi}^{\pi} \sqrt{1+\cos\alpha\cdot\sin 2\theta} \\ &\cdot e^{\frac{r\rho\cos(\theta-\theta_\rho)}{\psi_o\sin^2\alpha}} e^{\frac{\cos\alpha}{2\psi_o\sin^2\alpha}[r^2\sin 2\theta+\rho^2\sin 2\theta_\rho - 2r\rho\sin(\theta+\theta_\rho)]} \\ &\cdot \{e^{-g^2(r,\theta)} + \sqrt{\pi} g(r,\theta)[1+\operatorname{erf}(g(r,\theta))]\} d\theta, \\ &r \geq 0 \end{aligned} \tag{23a}$$

where

$$g(r,\theta) = \frac{\dot{\phi}_o\{\rho\sin(\theta-\theta_\rho) - \cos\alpha[r\cos 2\theta - \rho\cos(\theta+\theta_\rho)]\}}{\psi_o\sin\alpha\sqrt{2\beta(1+\cos\alpha\cdot\sin 2\theta)}}. \tag{23b}$$

β and $\dot{\phi}_o$ are defined by (11a) and (11d), respectively. A further investigation of the LCR $N_\xi(r)$ by substituting (11a)–(11d) in (23a) shows that $N_\xi(r)$ is proportional to the maximum Doppler frequency $f_{\max}$. Thus, the normalized LCR $N_\xi(r)/f_{\max}$ is independent of the vehicle speed and carrier frequency. The influence of the parameters κ_o, α, ρ, and θ_ρ on the normalized LCR $N_\xi(r)/f_{\max}$ can be studied from Fig. 5.

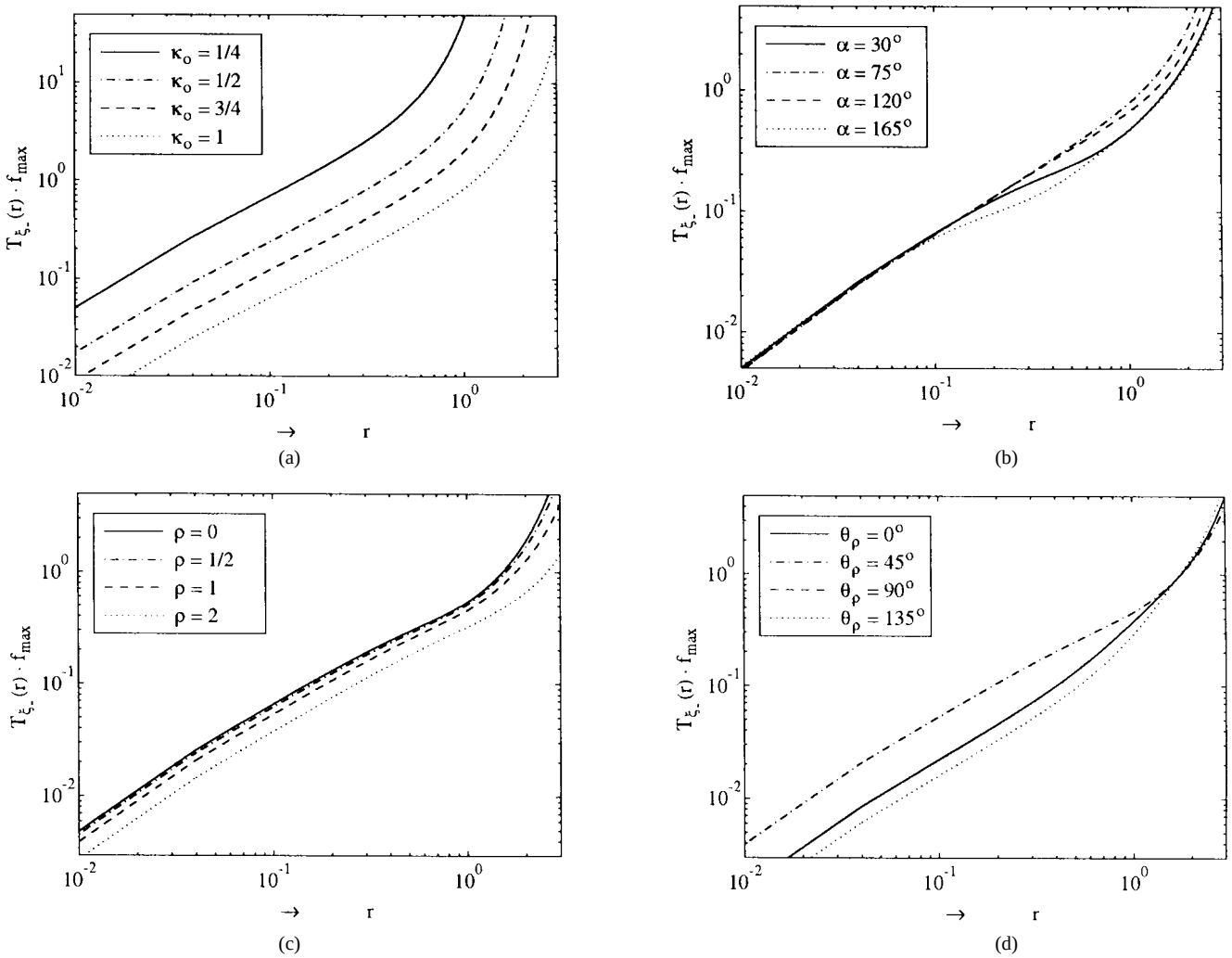

Fig. 6. Theoretical result of the normalized ADF $T_{\xi\_}(r)\cdot f_{\max}$ as a function of: (a) κ_o ($\sigma_o = 1,\ \alpha = 45^\circ,$ and $\rho = 0$), (b) α ($\psi_o = 1,\ \kappa_o = 1,$ and $\rho = 0$), (c) ρ ($\psi_o = 1,\ \kappa_o = 1,\ \alpha = 45^\circ,$ and $\theta_\rho = 45^o$), and (d) θ_ρ ($\psi_o = 1,\ \kappa_o = 1,\ \alpha = 45^\circ,$ and $\rho = 1$).

It can be shown that for the special case $\rho = 0$ and $\alpha \to 0^o$, (23a) reduces to the LCR of a one-sided Gaussian process, i.e.,

$$N_\xi(r) = \frac{\sqrt{\beta}}{\pi\sqrt{\psi_o}} e^{-\frac{r^2}{4\psi_o}}, \qquad r \geq 0 \tag{24}$$

where β is, in this case, given by $\beta = -\ddot{\psi}_o > 0$. Other special cases are of interest, e.g., if $\rho = 0$ and $\alpha = 90^o$, then $N_\xi(r)$ is proportional to the Rayleigh density [see (16)].

The ADF $T_{\xi\_}(r)$ is the expected value for the length of time intervals over which the signal envelope $\xi(t)$ is below a specified level r. In general, the ADF $T_{\xi\_}(r)$ is defined by [14]

$$T_{\xi\_}(r) = \frac{P_{\xi\_}(r)}{N_\xi(r)} \tag{25}$$

where $N_\xi(r)$ is the LCR of the process $\xi(t)$ and $P_{\xi\_}(r)$ indicates the probability that the process $\xi(t)$ is found below the level r. $P_{\xi\_}(r)$ can be derived from (13) according to

$$\begin{aligned} P_{\xi\_}(r) &= \int_0^r p_\xi(z)dz \\ &= \int_0^r \frac{z}{2\pi\psi_o \sin\alpha} e^{-\frac{z^2+\rho^2}{2\psi_o \sin^2\alpha}} \cdot \int_{-\pi}^{\pi} e^{\frac{z\rho\cos(\theta-\theta_\rho)}{\psi_o \sin^2\alpha}} \\ &\quad \cdot e^{\frac{\cos\alpha}{2\psi_o \sin^2\alpha}\cdot[z^2\sin 2\theta + \rho^2 \sin 2\theta_\rho - 2z\rho\sin(\theta+\theta_\rho)]} d\theta dz. \end{aligned} \tag{26}$$

Now, by substituting (23) and (26) into (25), the ADF $T_{\xi\_}(r)$ for the introduced process $\xi(t)$ [see (3)], with underlying cross-correlated quadrature components $\mu_1(t)$ and $\mu_2(t)$, can be evaluated. The influence of the parameters κ_o, α, ρ, and θ_ρ on the normalized ADF $T_{\xi\_}(r)\cdot f_{\max}$ can be studied from Fig. 6.

III. Modelling of Long-Term Fading Variations

In a typical mobile radio propagation situation, the local mean of the received signal is subjected to relatively slow variations. Such long-term variations are caused by shadowing effects, and it has been shown by many authors [3]–[5] that the local-mean value variations are lognormally distributed. The lognormal process, denoted here by $\zeta(t)$, can be derived from another real Gaussian noise process $\nu_1(t)$ with zero mean and unit variance according to

$$\zeta(t) = e^{s\nu_1(t)+m} \tag{27}$$

where s and m are two quantities determining the statistical properties of the local mean of the received signal. An analytical model for such a lognormal process is illustrated in Fig. 7. The process $\nu_1(t)$ is obtained by passing white Gaussian noise $n_1(t)$ with zero mean and unit variance through an ideal low-

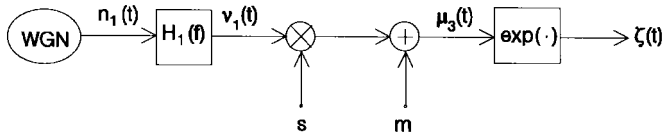

Fig. 7. Analytical model for lognormal processes, where $H_1(f) = \sqrt{S_{\nu_1\nu_1}(f)}$.

pass filter with transfer function $H_1(f) = \sqrt{S_{\nu_1\nu_1}(f)}$, where $S_{\nu_1\nu_1}(f)$ is the PSD function of the process $\nu_1(t)$. In this paper, we assume that $S_{\nu_1\nu_1}(f)$ is given by the Gaussian PSD function

$$S_{\nu_1\nu_1}(f) = \frac{1}{\sqrt{2\pi}\sigma_c} e^{-\frac{f^2}{2\sigma_c^2}} \tag{28}$$

where σ_c is related to the 3-dB cutoff frequency f_c according to $f_c = \sigma_c\sqrt{2\ln 2}$. Generally, f_c is much smaller than the maximum Doppler frequency $f_{\max}$. Therefore, it will be advantageous to introduce the quantity κ_c in order to express f_c by $f_c = f_{\max}/\kappa_c$.

The PDF of the lognormal process $\zeta(t)$, $p_\zeta(y)$, is defined by [15]

$$p_\zeta(y) = \begin{cases}$$

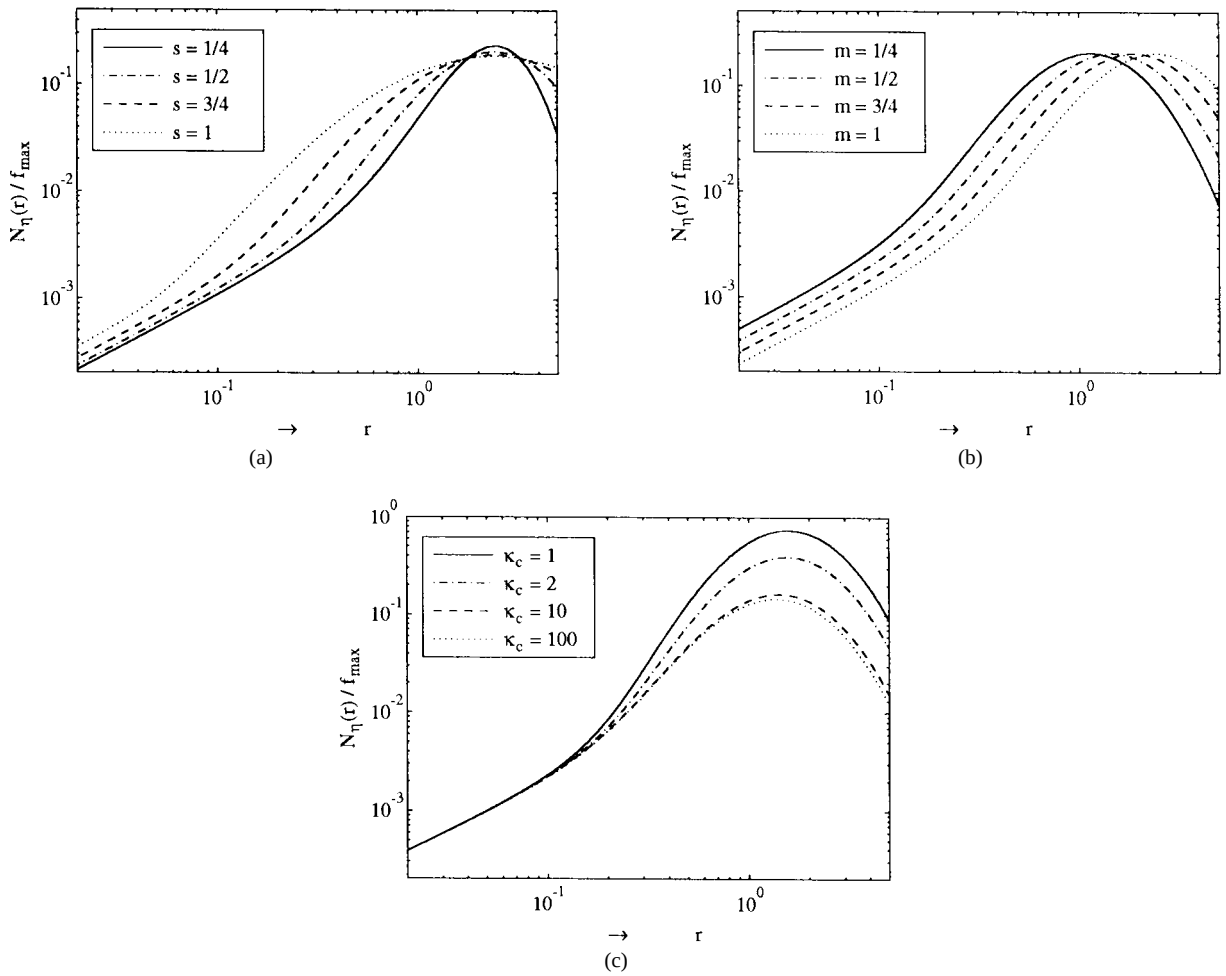

Fig. 9. Theoretical result of the normalized LCR $N_\eta(r)/f_{\max}$ as a function of: (a) s ($m = 1$ and $\kappa_c = 5$), (b) m ($s = 0.5$ and $\kappa_c = 5$), and (c) κ_c ($s = 0.5$ and $m = 0.5$), with $\kappa_o = 0.4553$, $\psi_o = 0.0412$, $\rho = 0.918$, $\theta_\rho = 86^o$, and $\alpha = 97^o$.

where $p_{\eta\dot{\eta}}(z,\dot{z})$ designates the JPDF of the extended Suzuki process $\eta(t)$ and its corresponding time derivative $\dot{\eta}(t)$ at the same time t. That JPDF can be derived by substituting $p_{\xi\dot{\xi}}(z,\dot{z})$ [see (22)] and $p_{\zeta\dot{\zeta}}(y,\dot{y})$ [see (30)] in the relation [9]

$$p_{\eta\dot{\eta}}(z,\dot{z}) = \int_o^\infty \int_{-\infty}^\infty \frac{1}{y^2} p_{\xi\dot{\xi}}(y,\dot{y}) \cdot p_{\zeta\dot{\zeta}}\left(\frac{z}{y}, \frac{\dot{z}}{y} - \frac{z}{y^2}\dot{y}\right) d\dot{y}dy, \quad z \geq 0\,. \tag{35}$$

The final result of the above equation can be expressed after some algebraic computations as follows:

$$\begin{aligned} p_{\eta\dot{\eta}}(z,\dot{z}) &= \frac{1}{(2\pi)^{3/2}\psi_o\sqrt{\beta}\sin\alpha} \int_o^\infty \frac{e^{-\frac{[\ln(z/y)-m]^2}{2s^2}}}{\sqrt{2\pi}s(z/y)^2} \cdot e^{-\frac{y^2+\rho^2}{2\psi_o \sin^2\alpha}} \\ &\cdot \int_{-\pi}^{\pi} \frac{e^{\frac{y\rho\cos(\theta-\theta_\rho)}{\psi_o\sin^2\alpha}} e^{\frac{\cos\alpha}{2\psi_o\sin^2\alpha}[y^2\sin 2\theta + \rho^2\sin 2\theta_\rho - 2y\rho\sin(\theta+\theta_\rho)]}}{h(y,\theta)\sqrt{1+\cos\alpha\cdot\sin 2\theta}} \\ &\cdot e^{-\frac{\left\{z - \frac{\dot{\phi}_o(z/y)[\rho\sin(\theta-\theta_\rho) - \cos\alpha(y\cos 2\theta - \rho\cos(\theta+\theta_\rho))]}{\psi_o\sin\alpha}\right\}}{2\beta(z/y)^2 h^2(y,\theta)(1+\cos\alpha\cdot\sin 2\theta)}} d\theta dy, \\ & z \geq 0. \end{aligned} \tag{36a}$$

with

$$h(y,\theta) = \sqrt{1 + \frac{\gamma(sy)^2}{\beta(1+\cos\alpha\cdot\sin 2\theta)}} \tag{36b}$$

where β, ψ_o, $\dot{\phi}_o$, and γ are defined by (11a), (11b), (11d), and (30b), respectively. After substituting (36) into (34), we obtain after some tedious algebraic computations the LCR of the extended Suzuki process $\eta(t)$, $N_\eta(r)$, as follows:

$$\begin{aligned} N_\eta(r) &= \frac{\sqrt{\beta}}{(2\pi)^2 s\psi_o\sin\alpha} \int_o^\infty e^{-\frac{[\ln(r/y)-m]^2}{2s^2}} \cdot e^{-\frac{y^2+\rho^2}{2\psi_o\sin^2\alpha}} \\ &\cdot \int_{-\pi}^{\pi} h(y,\theta)\sqrt{1+\cos\alpha\cdot\sin 2\theta} \cdot e^{\frac{y\rho\cos(\theta-\theta_\rho)}{\psi_o\sin^2\alpha}} \\ &\cdot e^{\frac{\cos\alpha}{2\psi_o\sin^2\alpha}[y^2\sin 2\theta + \rho^2\sin 2\theta_\rho - 2y\rho\sin(\theta+\theta_\rho)]} \\ &\cdot \left\{ e^{-\left[\frac{g(y,\theta)}{h(y,\theta)}\right]^2} + \sqrt{\pi}\frac{g(y,\theta)}{h(y,\theta)}\left[1 + \operatorname{erf}\left(\frac{g(y,\theta)}{h(y,\theta)}\right)\right]\right\} d\theta dy \end{aligned} \tag{37}$$

where $g(y,\theta)$ and $h(y,\theta)$ are the functions as defined by (23b) and (36b), respectively. A detailed investigation of (37) reveals that $N_\eta(r)$ is proportional to the maximum Doppler frequency $f_{\max}$. The influence of the parameters s, m, and κ_c on the normalized LCR $N_\eta(r)/f_{\max}$ can be studied from Fig. 9.

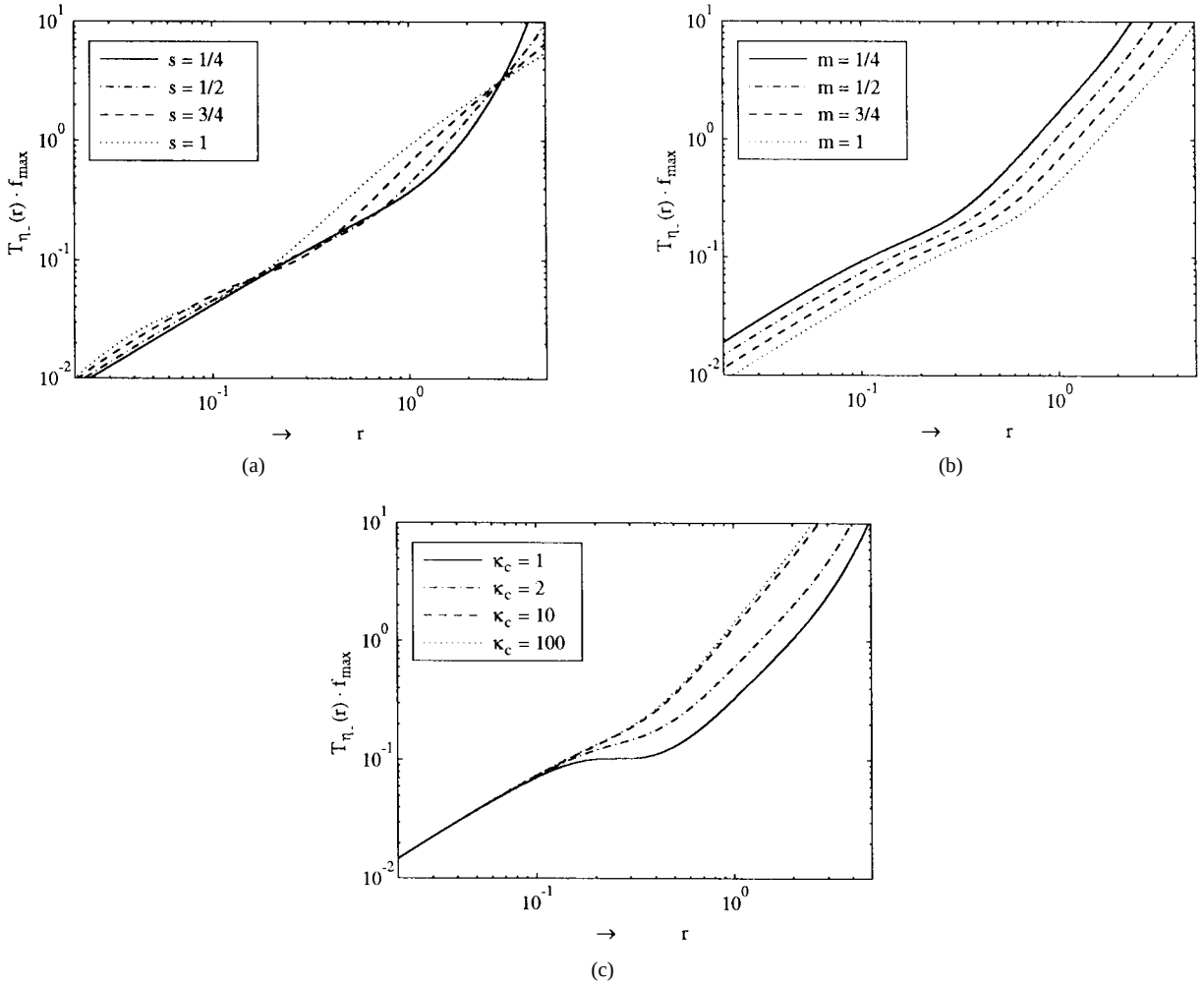

Fig. 10. Theoretical result of the normalized ADF $T_{\eta\_}(r) \cdot f_{\max}$ as a function of: (a) s ($m = 1$ and $\kappa_c = 5$), (b) m ($s = 0.5$ and $\kappa_c = 5$), and (c) κ_c ($s = 0.5$ and $m = 0.5$), with $\kappa_o = 0.4553$, $\psi_o = 0.0412$, $\rho = 0.918$, $\theta_\rho = 86°$, and $\alpha = 97°$.

The ADF of the extended Suzuki process $\eta(t)$, $T_{\eta\_}(r)$, can be expressed as

$$T_{\eta\_}(r) = \frac{P_{\eta\_}(r)}{N_\eta(r)} \tag{38}$$

where $P_{\eta\_}(r)$ is the cumulative distribution function (CDF) of the extended Suzuki process, which can be obtained by using (33) as follows:

$$P_{\eta\_}(r) = \int_o^r p_\eta(z)dz = \frac{1}{2\pi\psi_o \sin\alpha} \int_o^\infty \frac{y}{2} \left\{1 + \operatorname{erf}\left[\frac{\ln(r/y) - m}{s}\right]\right\} \cdot e^{-\frac{y^2+\rho^2}{2\psi_o \sin^2\alpha}} \cdot \int_{-\pi}^{\pi} e^{\frac{y\rho\cos(\theta-\theta_\rho)}{\psi_o \sin^2\alpha}} \cdot e^{\frac{\cos\alpha}{2\psi}}$$

TABLE I
OPTIMIZED PARAMETERS OF THE ANALYTICAL MODEL

Shadowing	σ_o	κ_o	α	ρ	θ_ρ	s	m	κ_c
Light	0.7697	0.4045	164°	1.567	127°	0.0052	−0.3861	1.735
Heavy	0.2774	0.506	30°	0.269	45°	0.0905	0.0439	119.9

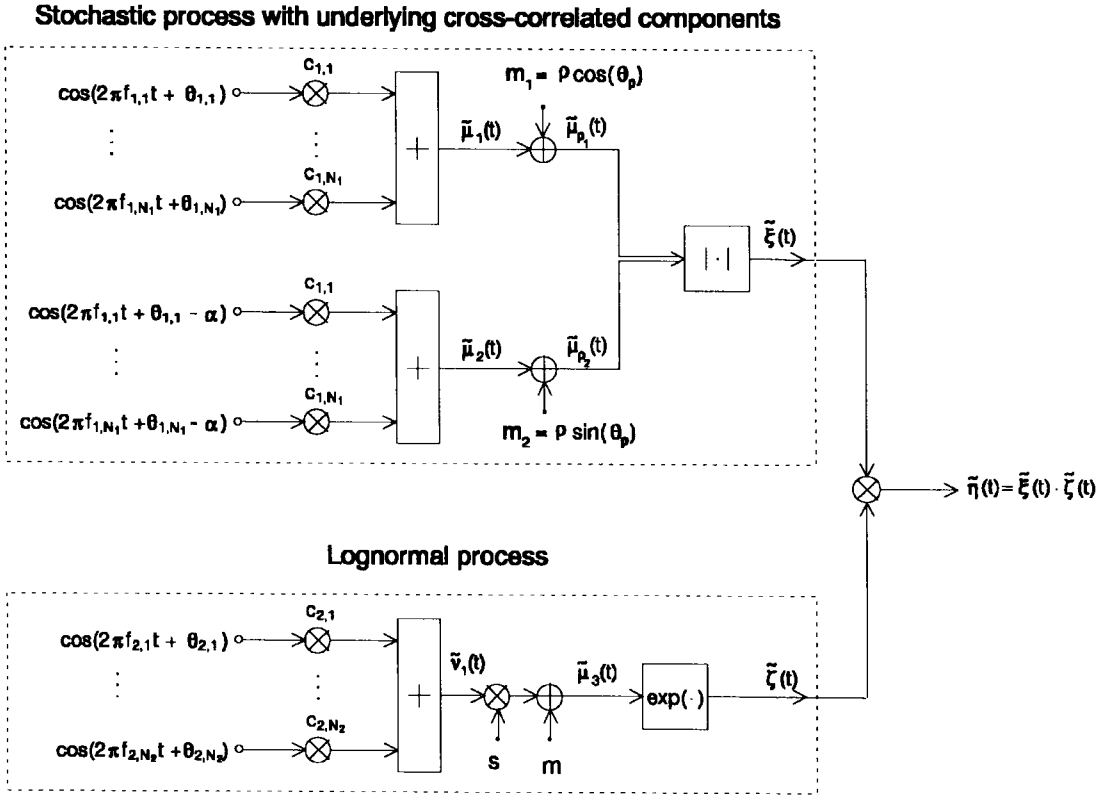

Fig. 11. Structure of the deterministic simulation system.

obtained reasonably good results, which are much better than the results shown in [11]–[13].

Next, we try to find optimal values for all the parameters $(\sigma_o, \kappa_o, \alpha, \rho, \theta_\rho, s, m,$ and $\kappa_c)$, which define the shape of the CDF $P_{\eta_+}(r) = 1 - P_{\eta_-}(r)$, the LCR $N_\eta(r)$, and the ADF $T_{\eta_-}(r)$. Therefore, we introduce the parameter vector $\mathbf{\Omega} = (\sigma_o, \kappa_o, \alpha, \rho, \theta_\rho, s, m, \kappa_c)$, and we minimize the following error function:

$$E_2(\mathbf{\Omega}) = \frac{1}{f_{\max}} \left\{ \sum_{m=1}^{M} \left[W_1\left(\frac{r_m}{\rho}\right) \left(N_\eta\left(\frac{r_m}{\rho}\right) - N_\eta^*\left(\frac{r_m}{\rho}\right) \right) \right]^2 \right\}^{\frac{1}{2}} + \left\{ \sum_{m=1}^{M} \left[W_2\left(\frac{r_m}{\rho}\right) \left(P_{\eta_+}\left(\frac{r_m}{\rho}\right) - P_{\eta_+}^*\left(\frac{r_m}{\rho}\right) \right) \right]^2 \right\}^{\frac{1}{2}} \tag{40}$$

where M is the number of measurement values and $W_1(\cdot)$ and $W_2(\cdot)$ are two appropriate weighting functions, which are defined by the reciprocals of $N_\eta^*(\cdot)$ and $P_{\eta_+}^*(\cdot)$, respectively. Observe that we only consider $N_\eta(\frac{r_m}{\rho})$ and $P_{\eta_+}(\frac{r_m}{\rho}) = 1 - P_{\eta_-}(\frac{r_m}{\rho})$ in the above error function, and we ignore $T_{\eta_-}(\frac{r_m}{\rho})$ because $T_{\eta_-}(\frac{r_m}{\rho})$ is completely defined by $P_{\eta_-}(\frac{r_m}{\rho})$ and $N_\eta(\frac{r_m}{\rho})$ [see (38)].

The minimization of (40) has been performed by applying the numerical optimization procedure proposed in [18]. The result of that procedure is shown in Table I, where for the equivalent satellite channel, the optimized parameters of the analytical model are listed.

In literature, the Rice factor $C = \rho^2/(2\psi_o)$ is often considered, which can be interpreted as the ratio of the power of the LOS component to that in the multipath (scattered) components. From Table I and by using (11b), we obtain for light shadowing $C_{dB} = 8.93$ dB and for heavy shadowing $C_{dB} = 1.435$ dB.

Now, let us replace in Figs. 1 and 7 the stochastical processes $\nu_o(t)$ and $\nu_1(t)$ by the following sums of sinusoids:

$$\tilde{\nu}_o(t) = \sum_{n=1}^{N_1} c_{1,n} \cos(2\pi f_{1,n} t + \theta_{1,n}) \tag{41a}$$

$$\tilde{\nu}_1(t) = \sum_{n=1}^{N_2} c_{2,n} \cos(2\pi f_{2,n} t + \theta_{2,n}) \tag{41b}$$

where $c_{i,n}$, $f_{i,n}$, and $\theta_{i,n}$ are called Doppler coefficients, discrete Doppler frequencies, and Doppler phases, respectively.

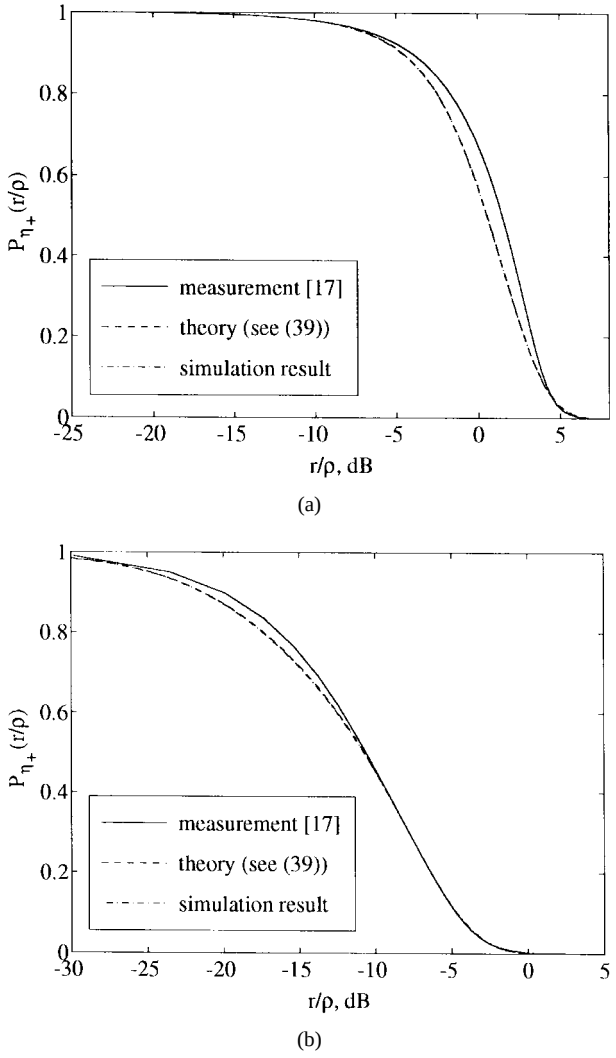

Fig. 12. CDF $P_{\eta_+}(r/\rho) = 1 - P_{\eta_-}(r/\rho)$ for: (a) light shadowing and (b) heavy shadowing.

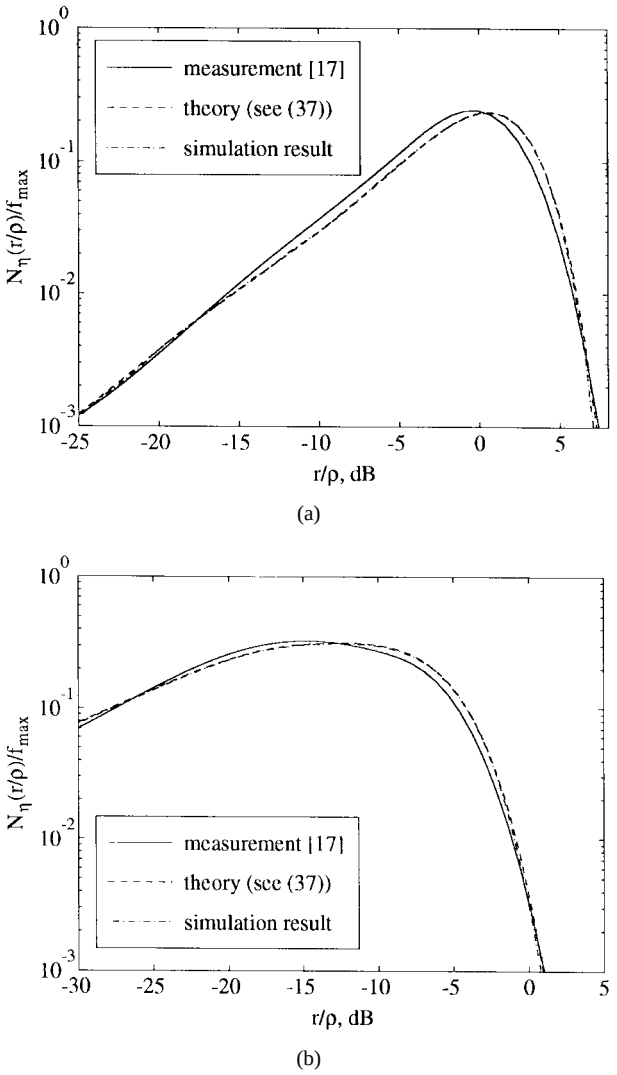

Fig. 13. Normalized LCR $N_\eta(r/\rho)/f_{\max}$ for: (a) light shadowing and (b) heavy shadowing.

In this manner, a proper deterministic simulation model for the proposed extended Suzuki model can be derived, which is shown in Fig. 11. By considering this figure, we observe then that an explicit realization of the Hilbert transformer has been avoided. A detailed introduction into the subject of deterministic simulation systems can be found in [19]–[22]. In this paper, we applied the method of exact Doppler spread presented in [20] and [22] to compute the discrete Doppler frequencies $f_{i,n}$ and the Doppler coefficients $c_{i,n}$. For the Jakes and Gaussian PSD, we have used $N_1 = 25$ and $N_2 = 15$ sinusoids, respectively. For the (restricted) Jakes PSD, the discrete Doppler frequencies $f_{i,n}$ are given by

$$f_{1,n} = f_{\max} \sin\left[\frac{\pi}{2N_1'}(n - \frac{1}{2})\right], \quad n = 1, 2, \ldots, N_1 \quad (42)$$

where $N_1' = \lceil \frac{N_1}{\frac{2}{\pi}\arcsin\kappa_c} \rceil$, and for the Gaussian PSD, the discrete Doppler frequencies $f_{2,n}$ are obtained by finding the zeros of

$$\frac{2n-1}{2N_2} - \operatorname{erf}\left(\frac{f_{2,n}}{f_{\max}}\kappa_c\sqrt{\ln 2}\right) = 0\,, \quad n = 1, 2, \ldots, N_2. \quad (43)$$

Equations (42) and (43) have been evaluated by using a maximum Doppler frequency $f_{\max}$ of $f_{\max} = 91$ Hz. The corresponding Doppler coefficients $c_{i,n}$ are given by

$$c_{i,n} = \begin{cases} \sigma_o\sqrt{\frac{2}{N_1'}}, & i = 1 \quad \text{(Jakes PSD)} \\ \sqrt{\frac{2}{N_2}}, & i = 2 \quad \text{(Gaussian PSD)}. \end{cases} \quad (44)$$

Finally, the Doppler phases $(\theta_{i,1}, \theta_{i,2}, \cdots, \theta_{i,N_i})$ can be simply identified with a permutation of the elements of the vector $\left(2\pi\frac{1}{N_i+1}, 2\pi\frac{2}{N_i+1}, \cdots, 2\pi\frac{N_i}{N_i+1}\right)$ for $i = 1, 2$. The number of samples N_s of the simulated output sequence $\tilde{\eta}(kT_a)$ was $N_s = 4 \times 10^6$, whereby a sampling interval T_a of $T_a = 1.8 \times 10^{-4}$s for light shadowing and $T_a = 3 \times 10^{-4}$s for heavy shadowing has been selected.

Fig. 12 shows a plot of the CDF $P_{\eta_+}(\frac{r}{\rho})$ for the analytical and simulation model. The measurement results are also shown. For heavy shadowing, the analytical model shows, in comparison with the measured values, little differences at low signal levels, but is in good agreement at high levels. While for the case of light shadowing, the results show reasonably good

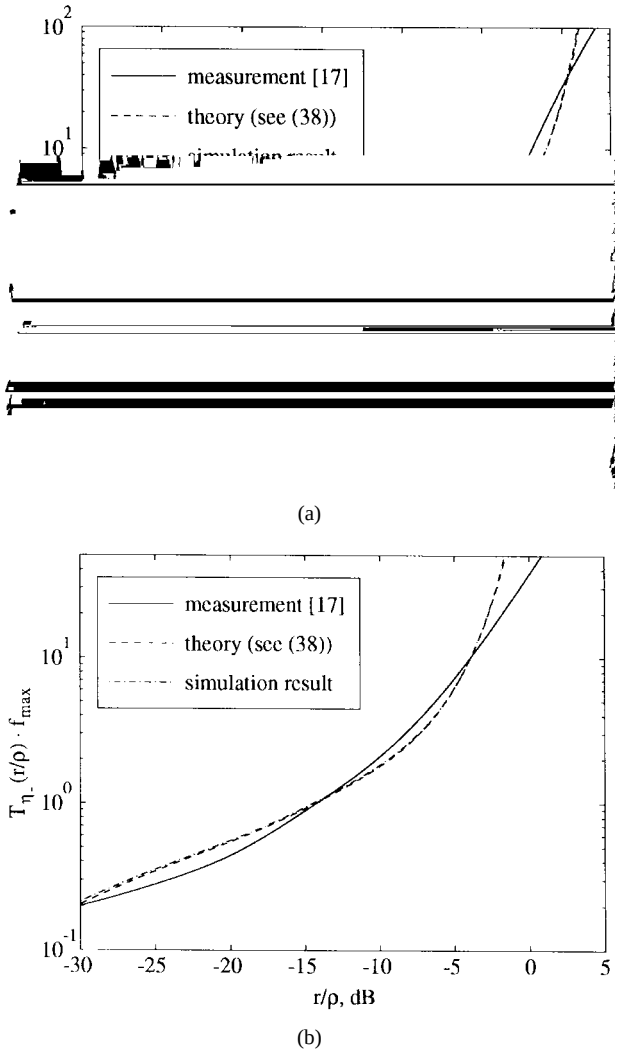

Fig. 14. Normalized ADF $T_{\eta\_}(r/\rho)\cdot f_{\max}$ for: (a) light shadowing and (b) heavy shadowing.

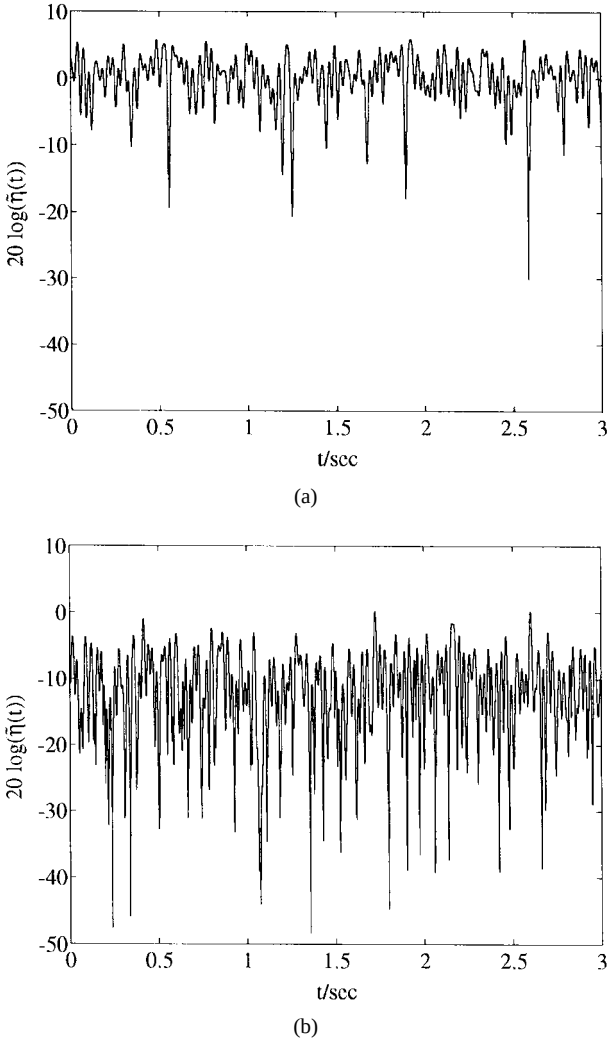

Fig. 15. Simulation of the envelope $\tilde{\eta}(t)$ for: (a) light shadowing and (b) heavy shadowing.

fits at low signal levels, but some deviations at median signal levels. For both cases, extremely good agreements between the analytical and simulation model were found throughout the entire signal range. Generally, results of both models, analytical and simulation, indicate a slightly higher fading behavior.

Fig. 13 shows a comparison of the normalized LCR's between the analytical model, simulation model, and measurement results. For light and heavy shadowing environments, the normalized LCR of the analytical model is in an extremely good agreement throughout all signal levels with the measurement data. For both models, analytical and simulation, Fig. 13 also shows that the corresponding normalized LCR's are nearly the same.

A comparison of the normalized ADF is shown in Fig. 14. Besides the differences in the low signal level for the case of light shadowing, the results of the analytical model are in fairly good agreement with the measurement data for both cases. Excellent fits are also found between the analytical model and the simulation model.

Finally, the resulting simulated envelopes $\tilde{\eta}(t)$ for light and heavy shadowing are presented in Fig. 15(a) and (b), respectively.

The results discussed above show that the analytical model can provide a good approximation of CDF, LCR, and ADF to measured values throughout the whole signal range. The proposed analytical model and corresponding deterministic simulation model for extended Suzuki processes should thus be useful for modeling and simulating of large classes of nonfrequency-selective land mobile radio channels.

VI. Conclusion

In this paper, we have introduced a new complex stochastical process, whose inphase and quadrature components are derived from a single colored Gaussian noise process. It has been shown that the absolute value, i.e., the amplitude (envelope), of this process contains the Rice, Rayleigh, and one-sided Gaussian process as special cases and, therefore, offers a greater flexibility than these classical stochastical processes. Consequently, the multiplication of the proposed process with the lognormal process results in an extension of the well-known Suzuki process, which is simply defined by the product of a Rayleigh and lognormal process. For this new type of extended Suzuki process, closed expressions for the amplitude pdf, LCR, and ADF have been derived. Several parameter

studies have demonstrated the highly flexible behavior of the analytical model, which allows, therefore, a good adaptation to the statistics of large classes of nonfrequency-selective mobile radio channels. This has been demonstrated successfully in the present paper by fitting the statistics of the extended Suzuki process to an equivalent real-world land mobile satellite channel for light and heavy shadowing environments. Finally, for the stochastic analytical model, a deterministic simulation model has been proposed whose statistical properties are in an excellent conformity with the analytical model as has been shown by various simulation results.

Both the proposed analytical and corresponding simulation model have constant parameters, and, thus, they are stationary models. An extension to modeling nonstationary satellite mobile channels can easily be performed by taking into account that the statistical properties of nonstationary channels can be approximated by an M-state Markow model, where each state represents a stationary channel model with different parameters [25]. For most experimental recordings, it would be enough to use a four-state Markow model [26].

REFERENCES

[1] R. H. Clarke, "A statistical theory of mobile radio reception," *Bell Syst. Tech. J.*, vol. 47, pp. 957–1000, July/Aug. 1968.

[2] M. J. Gans, "A power-spectral theory of propagation in the mobile radio enviroment," *IEEE Trans. Veh. Technol.*, vol. VT-21, pp. 27–38, Feb. 1972.

[3] D. O. Reudink, "Comparison of radio transmission at x-band frequencies in suburban and urban areas," *IEEE Trans. Antennas Propagat.*, vol. AP-20, pp. 470–473, July 1972.

[4] D. M. Black and D. O. Reudink, "Some characteristics of mobile radio propagation at 836 MHz in the Philadelphia area," *IEEE Trans. Veh. Technol.*, vol. VT-21, pp. 45–51, Feb. 1972.

[5] Y. Okumura, E. Ohmori, T. Kawano, and K. Fukuda, "Field strength and its variability in VHF and UHF land mobile radio services," *Rev. Electr. Commun. Lab.*, vol. 16, pp. 825–873, Sept./Oct. 1968.

[6] H. Suzuki, "A statistical model for urban radio propagation," *IEEE Trans. Commun.*, vol. COMM-25, no. 7, pp. 673–680, 1977.

[7] F. Hansen and F. I. Meno, "Mobile fading—Rayleigh and lognormal superimposed," *IEEE Trans. Veh. Technol.*, vol. VT-26, no. 4, pp. 332–335, 1977.

[8] A. Krantzik and D. Wolf, "Statistical properties of fading processes describing a land mobile radio channel" (in German), *Frequenz*, vol. 44, no. 6, pp. 174–182, June 1990.

[9] ———, "Distribution of the fading-intervals of modified Suzuki processes," *Signal Processing V: Theories and Applications*, L. Torres, E. Masgrau, and M. A. Lagunas, Eds. Amsterdam, The Netherlands: Elsevier, 1990, pp. 361–364.

[10] G. E. Corazza and F. Vatalaro, "A statistical model for land mobile satellite channels and its application to nongeostationary orbit systems," *IEEE Trans. Veh. Technol.*, vol. 43, no. 3, pp. 738–742, 1994.

[11] M. Pätzold, U. Killat, and F. Laue, "An extended Suzuki model for land mobile satellite channels and its statistical properties," submitted for publication.

[12] C. Loo, "A statistical model for a land mobile satellite link," *IEEE Trans. Veh. Technol.*, vol. VT-34, no. 3, pp. 122–127, 1985.

[13] C. Loo and N. Secord, "Computer models for fading channels with applications to digital transmission," *IEEE Trans. Veh. Technol.*, vol. 40, no. 4, pp. 700–707, 1991.

[14] W. C. Jakes, Ed., *Microwave Mobile Communications.* New York: IEEE Press, 1993.

[15] A. Papoulis, *Probability, Random Variables, and Stochastic Processes*, 3rd ed. New York: McGraw-Hill, 1991.

[16] S. O. Rice, "Mathematical analysis of random noise," *Bell Syst. Tech. J.*, vol. 23, pp. 282–332, July 1944 and vol. 24, pp. 46–156, Jan. 1945.

[17] J. S. Butterworth and E. E. Matt, "The characterization of propagation effects for land mobile satellite services," in *Int. Conf. Satellite Systems for Mobile Communication and Navigations*, 1983, pp. 51–54.

[18] R. Fletcher and M. J. D. Powell, "A rapidly convergent descent method for minimization," *Comput. J.*, vol. CJ-6, no. 2, pp. 163–168, 1963.

[19] M. Pätzold, U. Killat, and F. Laue, "A deterministic digital simulation model for Suzuki processes with application to a shadowed Rayleigh land mobile radio channel," *IEEE Trans. Veh. Technol.*, vol. 45, no. 2, pp. 318–331, 1996.

[20] M. Pätzold, U. Killat, F. Laue, and Y. Li, "A new and optimal method for the derivation of deterministic simulation models for mobile radio channels," in *Proc. IEEE Veh. Technol. Conf., VTC '96*, Atlanta, GA, pp. 1423–1427.

[21] M. Pätzold, U. Killat, Y. Shi, and F. Laue, "A deterministic method for the derivation of a discrete WSSUS multipath fading channel model," *European Trans. Telecommun.*, vol. ETT-7, no. 2, pp. 165–175, Mar./Apr. 1996.

[22] M. Pätzold, U. Killat, F. Laue, and Y. Li, "On the statistical properties of deterministic simulation models for mobile fading channels," submitted for publication.

[23] D. Parson, *The Mobile Radio Propagation Channel.* London: Pentech, 1992.

[24] I. S. Gradstein and I. M. Ryshik, *Tables of Series, Products, and Integrals*, vols. 1 and 2. Thun: Harri Deutsch, 1981.

[25] B. Vucetic and J. Du, "Channel modeling and simulation in satellite mobile communication systems," *IEEE J. Select. Areas Commun.*, vol. 10, no. 8, pp. 1209–1218, 1992.

[26] ———, "Channel modeling and simulation in satellite mobile communication systems," in *Proc. Int. Conf. Satellite Mobile Commun.*, Adelaide, Australia, 1990, pp. 1–6.

Matthias Pätzold (M'94) was born in Engelsbach, Germany, in 1958. He received the Dipl.-Ing. and Dr.-Ing. degrees in electrical engineering from Ruhr University, Bochum, Germany, in 1985 and 1989, respectively.

From 1990 to 1992, he was with ANT Nachrichtentechnik GmbH, Backnang, where he was engaged in digital satellite communications. Since 1992, he has been Chief Engineer at the Digital Communication Systems Department of the Technical University Hamburg-Harburg, Hamburg, Germany. His current research interests include mobile communications, especially multipath fading channel modeling, channel parameter estimation, and channel coding theory.

Ulrich Killat (M'91) received the diploma and Ph.D. degrees from the University of Hamburg, Hamburg, Germany, in 1969 and 1973, respectively.

He worked in the research laboratories of Philips in Hamburg and Aachen, Germany. Since 1991, he has been Professor and Head of the Department of Digital Communication Systems at the University of Hamburg-Harburg, Hamburg. His research interests include traffic theory, coding theory, and modeling and simulation of communication networks.

Yingchun Li was born in Shanghai, China, in 1962. He received the B.S.E.E. degree from the Shanghai University of Science and Technology, Shanghai, China, in 1984.

Since 1984, he has been with the Modern Communication Group of the Shanghai University of Science and Technology, where he is engaged in optical fiber and digital communication. From 1995 to 1996, he was a Visiting Scholar at the Digital Communication Systems Department of the Technical University of Hamburg-Harburg, Hamburg, Germany, where he worked on modeling of mobile communication channels. His current research interests include mobile and personal communication systems as well as hybrid fiber-coaxial networks.

Frank Laue was born in Hamburg, Germany, in 1961. He received the Dipl.-Ing. (FH) degree in electrical engineering from the Fachhochschule, Hamburg, in 1992.

Since 1993, he has been CAE-Engineer at the Digital Communication Systems Department of the Technical University of Hamburg-Harburg, Hamburg, where he is involved in mobile communications.